SYNTHESIS OF AG^0 NANOPARTICLES FROM EXTRACT AND ETHANOLIC AND AQUEOUS FRACTIONS OF LEAVES AND PETALS OF *HIBISCUS ROSA-SINENSIS* L.

SAYES REÁTEGUI CAROLINA G.[*], *HERRERA HERNÁNDEZ NORA AND HUAROTE EMILY*

Green Chemistry and Biotechnology Research Laboratory. Faculty of Natural Sciences and Mathematics. Research, Development and Innovation Group in Green Chemistry and Biotechnology (GIDIVEB). Federico Villarreal National University (UNFV). Lima Peru.

ABSTRACT

The synthesis of nanoparticles from plant extracts has become an interesting line of research in recent years. The purpose of the study was the synthesis of silver nanoparticles (AgNPs) from silver nitrate, aqueous and ethanol 80% extracts obtained by ultrasound-assisted extraction, as well as fractions of chloroform, ethyl acetate and water, of flower petals and leaves of *Hibiscus rosa-sinensis* L. The ethanolic extract of petals of *H. rosa-sinensis* L. was analyzed by UHPLC-ESI-Q-Orbitrap- MS/MS identifying pelargonidin, petunidin, kaempferol, and orientin. Characterization of AgNPs by UV-Visible spectrophotometry gave a λ_{max} at 400,631 nmand 389,411 nm for AgNPs obtained with ethanolic extract of flower petals and leaves, λ_{max} at 402,270 nm and 391,057 nm for AgNPs of aqueous extracts of flower petalsand leaves respectively. FTIR confirmed the reduction of Ag^+ ions to Ag^0 ions in AgNPS. Dynamic light dispersion (DLS) showed an effective diameter of the AgNPS from extracts, less than 80 nm and for AgNPs from fractions was less at 53 nm and near-zero polydispersity indices. Electron field emission scanning microscopy (FE-SEM) showed a particle size between 17 - 32 nm for AgNPs from extracts, and 15 - 26 nm for AgNPs from fractions, which showed a spherical structure. X-ray Diffraction (XRD) and Energy Dispersive Spectroscopy (EDS) analysis confirmed the elemental composition of AgNPs showing mostly silver (60.44%), oxygen (32.48%) and potassium (4.97%). This study revealed that the compounds from the extracts of *Hibiscus rosa-sinensis* L. are good reducing and stabilizing agents for the synthesis of silver nanoparticles, being pH 9 optimal for synthesis.

Keywords: Green synthesis, *Hibiscus rosa-sinensis*, FE-SEM, UHPLC, nanoparticles.

INTRODUCTION

In recent years the area of nanotechnology has had a great environmental and health impact due to its applications for the removal of heavy metals in water [1] and its antimicrobial activity [2].

The synthesis of silver nanoparticles has been extensively studied using chemical and physical methods, however, such methods have a considerable environmental impact, are technically laborious and economically costly [3].

At present, the great challenge for chemistry is the synthesis of compounds generating the minimum possible environmental impact, since most of the reagents used for synthesis are organic compounds that produce toxic wastes for the environment and health, such as excess carbon dioxide in the atmosphere, water pollution, damages that directly affect the population and are high impact [4].

The current trend is to develop green preparation technologies and reduce the emission of harmful substances in the production process [5] "green" ecological processes in chemistry and chemical technologies are becoming increasingly popular and much needed due to global environmental problems [6]. The application of natural products is taking relevance in this aspect since they promote a green synthesis, are eco-friendly with the environment, have low toxicity, are low cost and are very efficient.

The benefit of using *Hibiscus rosa-sinensis L* is to obtain stable Ag^0 nanoparticles by an eco-friendly technique.

EXPERIMENTAL

A. Chemicals

Silver nitrate (Sigma; purity >99%), 96% ethanol, ultrapure water, and potassium hydroxide (Sigma; purity >90%) were used.

B. Samples

Plant samples of leaves and petals of *Hibiscus rosa-sinensis* were collected in the gardens of the Universidad Nacional Federico Villarreal, Peru in August 2019. The taxonomic identification of the plant material was carried out at the Natural History Museum of the Universidad Nacional Mayor de San Marcos, Lima, Peru (UNMSM) with the constancy N° 406 - USM - 2019.

C. Instruments

The UV/VIS UV single-beam spectrophotometer was used for the identification of possible flavonoids in raw extract and the characterization of AgNPs obtained from extracts and fractions. The infrared spectrophotometer (FTIR) was used to identify the links formed by the AgNPS with the extracts obtained, both teams are in the Laboratory of Experimental Chemistry of the National University Federico Villarreal.

The identification of organic compounds was carried out with the UHPLC-ESI-Q-Orbitrap-MS/MS reverse phase C-18 equipment and the Thermo Scientific SIEVE software used for data collection, both located in the laboratory of Natural Products of the University of Antofagasta, Chile.

D. Extract preparation

The plant material (leaves and flowers) of *Hibiscus rosa-sinensis L* was selected [7] washed, disinfected [8], dried at 40°C [9] and was pulverized with a blade mill obtaining 20.7 g of leaves and 16.3 g of flower petals.

The dried and ground leaves and petals (5 g) were extracted separately with 50 mL of 80% ethanol (EtOH) [10], by ultrasound at 25° C for 10 minutes three times [9], [11]. The aqueous extracts were obtained from 5 g of leaves and petals of *H. rosa-sinensis* L. and 100 mL of ultrapure boiling water [12], [13]. The extracts obtained, ethanolic and aqueous, were filtered with Whatman filter paper [10] and concentrated in a range of 37 to 39°C.

E. Fractionation of EtOH extracts of leaves and petals of *H. rosa-sinensis* L.

EtOH extracts of leaves and flowers were defatted with petroleum ether [14], [15] and fractionated with solvents in increasing polarity: chloroform (C), ethyl acetate (AE) and water (A) [16]

F. Phytochemical analysis and TLC

The dried plant material powder of leaves and petals of *H. rosa-sinensis* L. was analyzed by phytochemical screening to detect the presence of polyphenolic compounds, tannins, flavonoids and terpenoids [17].

Thin-layer chromatography (TLC) was also performed on ethanolic extracts and fractions obtained using silica gel-coated chromatoplates 60 as stationary phase and BAW (BuOH - AcOH - H_2O, 3:1:1), as mobile phase. The plates were visualized with vanillin-H_2SO_4 heated at 110°C.

*Corresponding author email: ginn_sr@outlook.com

G. Analysis of EtOH extract by UHPLC-ESI-Q-Orbitrap-MS/MS

An aliquot of the EtOH extract of *H. rosa-sinensis* L. was analyzed by an Ultra-High-Performance Liquid Chromatography- Electrospray ionization - Quadrupole -Orbitrap - Mass Spectrometry (UHPLC-ESI-Q-OrbitrapMS-MS) Reverse Phase C-18, coupled to a Mass Spectrophotometer (THERMO Q-Exactive) with quadrupole precursor, operated in Electro-Spray mode with positive ionization (ES+) [18].

The flow of the mobile phase - 1mL/min and the stroke time for 35 min, the volume of the injected sample being 10 µL. The composition of the mobile phase was 95% water and 5% acetonitrile.

H. Green synthesis of AgNPs

AgNPs - Ag from extracts

The EtOH and aqueous extracts (12 mL) obtained from leaves and petals of *Hibiscus rosa-sinensis L.*, were carried at different pH (7, 9, 11 and 13) with a solution of KOH 2 M, under agitation [8]. Subsequently, the $AgNO_3$ solution was added in different concentrations (0.08 mmol L-1 and 0.8 mmol L-1) and stirred until colour variation was displayed.

AgNPs - Ag from fractions

Each of the fractions of chloroform (C), ethyl acetate (AE) and aqueous (A) obtained from of leaves and petals of *Hibiscus rosa-sinensis* L. were taken to dryness (0.2 g) and dissolved in 20 mL of ultrapure water [19]. An aliquot of 12 mL was carried at pH 9 using KOH 2 M [8] and a solution of $AgNO_3$ 0.8 mmol L^{-1} was added under permanent agitation until colour variation.

I. Characterization of AgNPs

The AgNPs were analyzed by UV-VIS spectroscopy using a quartz cell, at room temperature (25°C), in a range of 200-600 nm [8]. Then Dynamic Light Scattering (DLS) analysis was performed to obtain the effective diameter of AgNPs [1].

Field Emission Scanning Electron Microscopy (FE-SEM) was used to determine the shape and size of AgNPs. This technique allows obtaining results of topology, chemical composition and crystalline structure [20]. Additionally, the analysis was performed by X-ray Diffraction (XRD) and Energy Dispersive Spectroscopy (EDS) technique, which is a complement to FE-SEM and allows determining the elemental composition of AgNPs [21]. Finally, infrared spectrometry with Fourier Transform Infrared Spectroscopy (FTIR), to identify the bonds formed by the functional groups present in the extracts and the synthesized AgNPs [22], [23].

RESULTS AND DISCUSSION

In the research, the AgNPs were synthesized using extracts and fractions from leaves and petals of *Hibiscus rosa-sinensis* L., which can act both as reducing agents and as stabilizing agents [24].

Phytochemical analysis

The results for the detection of polyphenolic compounds, tannins, flavonoids and terpenoids with preliminary phytochemical screening are presented in Table 1.

Table 1. Preliminary phytochemical analysis of *Hibiscus rosa-sinensis* L.

Test	A	B	C	D
$FeCl_3$	+	+	+	+
Shinoda Test	-	-	+	+
Liebermann-Burchard Test	+	+	+	+
Gelatin-Salt test	+	+	+	+

(+) = Positive; (-) = Negative

Aqueous extract of leaves (A) and petals (B); ethanolic extract of leaves (C) and petals (D)

Flavonoids and polyphenolic compounds were detected in ethanolic extracts of leaves and petals, which was verified by thin layer chromatography (TLC) with silica gel 60, BAW (BuOH - AcOH – H_2O, 3:1:1) and vanillin-H_2SO_4 developer.

In the ethanolic extract (EtOH) of the petals, dark green spots were observed at 365 nm, with Rfs between 3.5 and 5.5, characteristic of isoflavones, flavonols and flavones, which coincided with those found in another species of the genus Hibiscus, then it was analyzed EtOH extract by UHPLC-ESI-Q-Orbitrap-MS/MS.[25]

Analysis by UV-Vis spectrophotometry extracts

A preparative TLC was performed with the ethanolic extracts of leaves and petals, the fractions obtained were analyzed in UV-visible, giving λ_{max} 327.041 nm with a shoulder of 269.019 nm for leaves extract and λ_{max} of 345.035 nm with a shoulder of 264.695 nm, for the extract of petals. The signals in the spectrum appear between 250 and 370 nm, a typical region of phenolic groups [26], confirming the reducing capacity of both extracts due to the presence of phenolic groups [27], [28].

Analysis by UHPLC-ESI-Q-Orbitrap-MS/MS

Analysis by UHPLC-ESI-Q-Orbitrap MS-MS of the EtOH extract of the flower petals of *Hibiscus rosa-sinensis* L provided the molecular weight of the structures present.

Table 2. Secondary metabolites identified in UHPLC-ESI-Q-Orbitrap-MS-MS.

Possible compound	Comp. elemental [M-H]	Rt. (min.)	Theoretical mass (*m/z*)	Reference mass	Mass exp. (*m/z*)
Peonidin	$C_{16}H_{13}O_6^-$	9.94	301.0706	301*	301.0749
Pelargonidin	$C_{15}H_{11}O_5$	9.31	271.0600		271.0595
Kaempferol	$C_{15}H_8O_7^-$	13.24	285.0404	285*	285.0405
Gossypin	$C_{21}H_{19}O_{13}^-$	13.37	479.0827		479.0825
Astilbin	$C_{21}H_{21}O_{11}^-$	14.41	449.1086	449.1089**	449.1083
Orientin	$C_{21}H_{19}O_{11}^-$	16.70	447.0931	447*	447.0927

*****[29], ****** [30]

The flavonoids pelargonidin [31], [32], peonidin [33], kaempferol [34], [35], orientin [36], astilbin [37], [38], gossypin [39], were identified in the ethanolic extract of the petals of *H. rosa-sinensis* L (Table 2). Compound 3 showed a fragment of m/z 285, which corresponds to the mass of kaempferol as aglycone, while the difference (308) corresponds to the loss of a rutinoside (glucose-nose disaccharide), which indicates the presence of the kaempferol rutinoid, which has already been notified [35]. Although this information does not rule out the possibility that aglycone is luteolin rather than kaempferol. These compounds be reducing and stabilizing agents in the formation of the nanoparticles [8], [13], [40], [41].

Green synthesis of AgNPs

The synthesis of AgNPs with the extracts of *Hibiscus rosa sinensis* L. at pH 7, 9 and 11 formed the AgNPs from S1 to S12 (Table 3). At pH 13 there was precipitation [43] due to the possible formation of larger particles

Table 3. AgNPs synthesized from extracts of leaves and petals at pH 7, 9 and 11.

Extracts	Vegetal drugs	pH	Code
Ethanolic	Petals	7	S1
	Leaves		S2
Aqueous	Petals		S3
	Leaves		S4
Ethanolic	Petals	9	S5
	Leaves		S6
Aqueous	Petals		S7
	Leaves		S8
Ethanolic	Petals	11	S9
	Leaves		S10
Aqueous	Petals		S11
	Leaves		S12

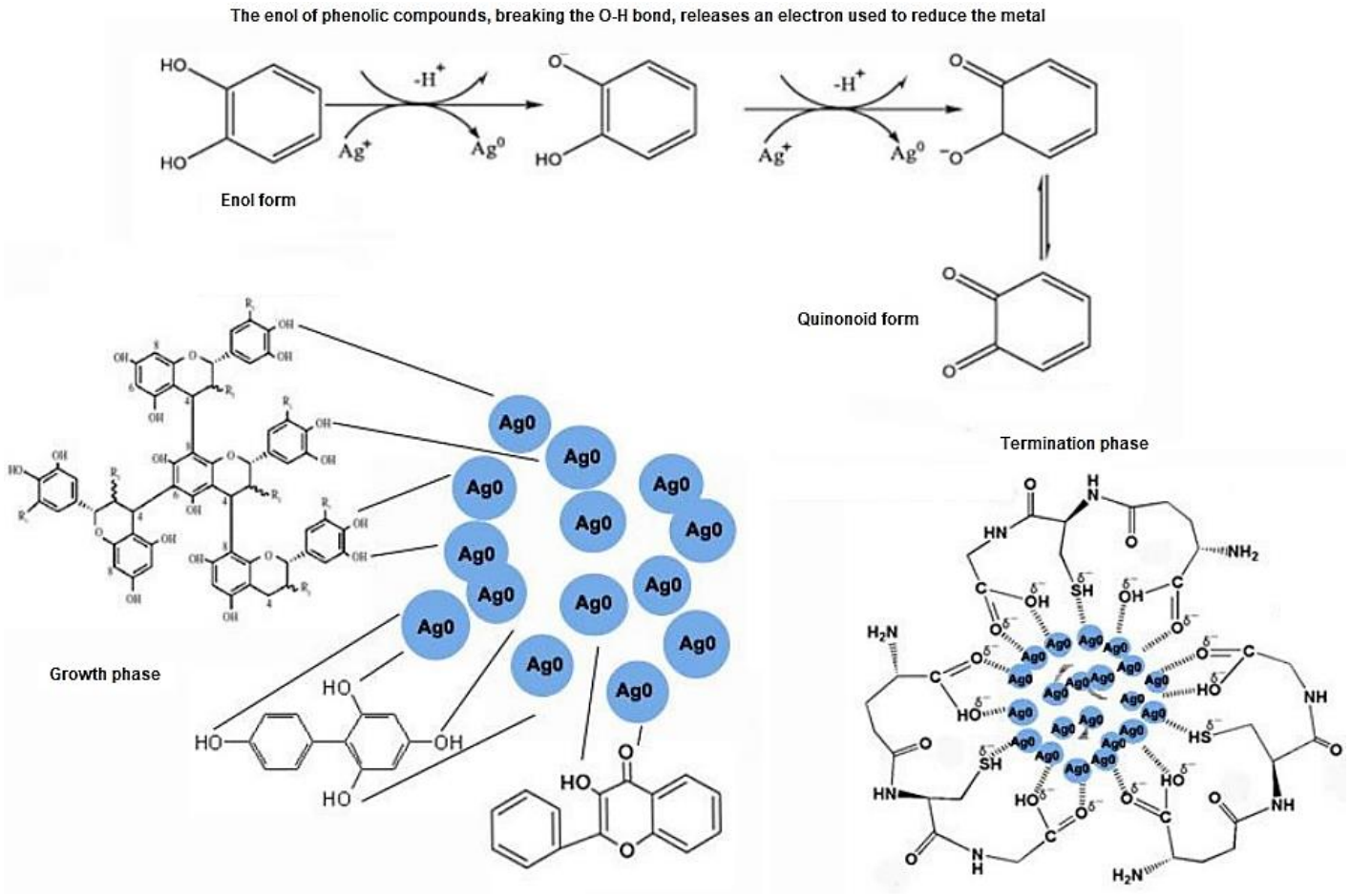

Figure 1. The probable mechanism of bio-reduction and stabilization to form nanoparticles [42].

Table 3 shows all the AgNPs obtained with the extracts at pH 7, 9 and 11. At pH 13, precipitation [43] was demonstrated due to the possible formation of larger particles, so they were not analyzed further.

The formation of AgNPs by reduction of Ag^{+1} to Ag^0 (Figure 1) when combined with the reducing compounds of the extracts (leaves or petals) was evidenced by the immediate change from pale yellow to intense orange (leaves) and orange yellow (petals) [41]. The intensity of the final color also varied according to pH.

The AgNPs obtained (S13 to S18) from the chloroform (C), ethyl acetate (AE) and aqueous (A) fractions of leaves and petals are shown in Table 4. The AgNPs S13, S15, S17 and S18, presented a color change from pale yellow to yellow-orange, similar to the AgNPs obtained with the extracts. However, the AgNPs S14 and S16 showed a color from pale yellow to intense yellow and with time the yellow color disappeared, this may be due to the fact that most of the phenolic compounds, in the leaves, are found in the aqueous fraction of higher polarity [44].

Table 4. AgNPs synthesized from fractions of leaves and petals at pH 9.

Fraction	Vegetal drugs
Chloroformic (C)	Petals
	Leaves
Ethyl acetate (AE)	Petals
	Leaves
Aqueous (A)	Petals
	Leaves

Characterization of AgNPs

UV-Vis spectrophotometry was used to determine the presence of chromophore groups and aromatic rings in the extracts, measuring the electronic transition of π bonds, σ bonds and free electron pairs.

Table 5. UV Vis spectral assignment of the aqueous and ethanol extracts of leaves and petals of *Hibiscus rosa-sinensis* L.

Samples	(λ_{max}) nm	Abs
S1	408.713	0.320
S2	-	-
S3	401.060	0.309
S4	409.10	0.439
S5	400.631	0.725
S6	389.411	1.240
S7	402.270	0.614
S8	391.057	0.601
S9	397.419	0.262
S10	-	-
S11	402.006	0.294
S12	383	0.366

The plasmon surface for the absorption bands of AgNPs is between 300 to 600 nm [45], but the closer to the extremes, the more easily AgNPs could precipitate, the optimal range being 390 to 450 nm. Plasmon resonance values between 390 and 410 nm were obtained for AgNPs synthesized from *Hibiscus rosa sinensis* L. extracts (Table 5), which would confirm the reduction of Ag^{+1} to Ag^0 [13], [41] The Surface Plasmon Vibration (SPR) is presented by the resonance phenomenon that occurs in metallic nanoparticles [46], and also evidences the stability of AgNPs.

Table 6. UV Vis spectral assignment of the AgNPs from C, AE, A fractions of leaves and petals of *Hibiscus rosa-sinensis L.* to pH 9.

Samples	(λ_{max}) nm	Abs
S13	209.606	4.073
S14	-	-
S15	407.033	1.628
S16	-	-
S17	402.696	2.232
S18	386.068	1.280

The SPR in the UV-Vis region of the spectrum originates from the resonant collective oscillations of conduction electrons along the transverse direction of the electromagnetic field. The maximum intensity of the SPR band and the bandwidth are influenced by the shape of the particles, the narrower the bandwidth, the more stable they will be and will present a smaller size [47]. Tables 6 show the (λ_{max} max) nm and absorbences of AgNPs synthesized with extracts and leaves fractions and petals of *H. rosa-sinensis* L. respectively.

The shape and size of the nanoparticles cause more intense and narrow absorption bands, if they are close to monodispersion (defined size of nanoparticles), however, if the band is wider and less intense, it is closer to polydispersity (nanoparticles). of different sizes). The most intense and narrow absorption band obtained was for AgNPs S5 (Figure 2) at pH 9, which would be the most suitable pH for AgNPs synthesis.

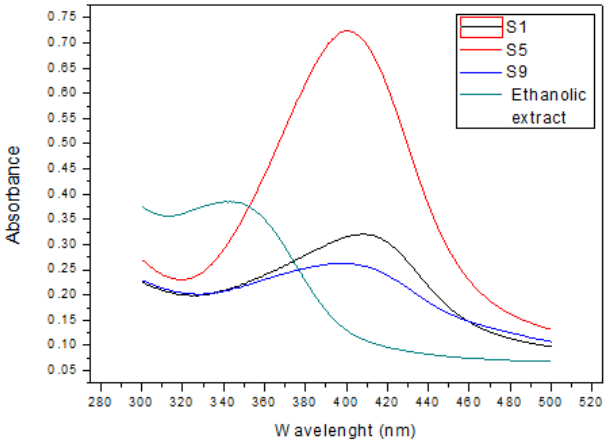

Figure 2. UV-visible spectra of AgNPs (S1, S5 and S9) and ethanolic extract of *Hibiscus rosa sinensis* L. petals.

From the analysis of the AgNPs obtained at pH 9 with the fractions of chloroform (C), ethyl acetate (AE) and water (A) from leaves and petals of *Hibiscus rosa sinensis L.* (Figure 3), it was observed that the band of more intense absorption was for the AgNP S17 unlike the AgNPs S13 and S15.

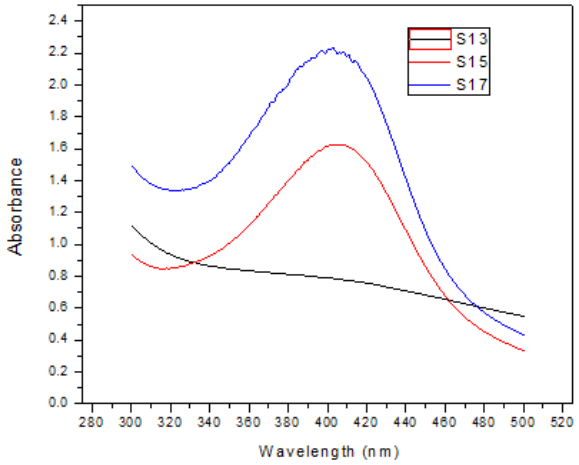

Figure 3. UV-visible spectra of AgNPs (S13, S15 and S17) of *Hibiscus rosa sinensis* L. petals.

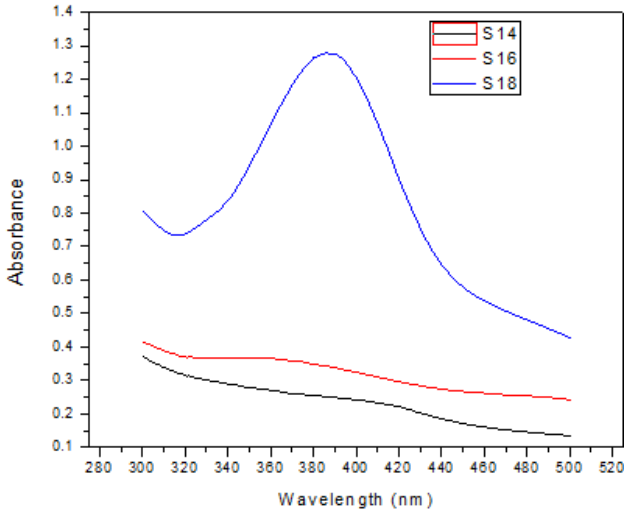

Figure 4. UV-visible spectra of AgNPs (S14, S16 and S18) of *Hibiscus rosa sinensis L.* leaves.

The AgNPs S14 and S16 (Figure 4) do not show signals in Uv-Vis due to the fact that possibly the chloroform (C) and ethyl acetate (AE) fractions of *Hibiscus rosa sinensis* L. leaves do not have the presence of reducing agents. Most of the reducers and stabilizers of AgNPs (polyphenols) are found in the aqueous fractions of leaves and petals [48].

The effective diameters and polydispersity indices of the AgNPs (Tables 7 and 8) were obtained with the dynamic light scattering (DLS) method.

Table 7. Effective diameters (nm) and polydispersity index by the dynamic light scattering method of AgNPs (S1 to S12) of leaves and petals of *Hibiscus rosa- sinensis* L.

Samples	Effective diameter (nm)	Polidispersity Index
S1	32.1	0.301
S2	108.3	0,311
S3	66.1	0.317
S4	152.6	0.317
S5	52.5	0.346
S6	49.9	0.285
S7	39.8	0.270
S8	75.4	0.368
S9	63.5	0.354
S10	86.0	0.290
S11	229.1	0.386
S12	108.5	0.315

AgNPs S6 and S7 have mono dispersion and can be observed in the size of NPS giving a diameter less than 50 nm, demonstrating that synthesis is more efficient at a medium alkaline pH, due to the ability of the medium to change the electrical charges of biomolecules, improving the reducing and stabilizing capacity of polyphenolic compounds present in extracts and fractions [13], [49].

Table 8. Effective diameter (nm) and polydispersity index by the dynamic light scattering method of AgNPs (S13 to S18) of leaves and petals of *Hibiscus rosa- sinensis* L.

Samples	nm	Polidispersity Index
S13	271.1	0.224
S14	-	-
S15	262.0	0.306
S16	-	-
S17	25.7	0.281
S18	42.0	0.227

The analysis of the nanoparticles (S13 to S18) synthesized at pH 9 gave an effective diameter in a range of 25.7 nm to 272 nm (Table 8). The smallest effective diameter was identified in S17 with 25.7 nm; however, it can be observed that for S18 the variation in size is considerable with 42.0 nm. The size of the AgNPs of S13 and S15 showed a size of 271.1 nm and 262.0 nm, respectively.

The AgNPs (S14 and S16) did not present a signal in DLS, possibly because their size is greater than 500 nm [50]. It also confirms that the highest amount of polyphenols are found in the extract and in the petal fractions of *Hibiscus rosa-sinensis* [11], [51]. In the leaves, the highest concentration of polyphenols is found in the aqueous fraction (A) [48].

The polydispersity indices close to zero, according to Alvear et al., 2017, show that the AgNPs probably present homogeneity in size, which would prevent them from agglomerating and precipitating. [22], [53].

The FE-SEM analysis allowed us to determine that the AgNPs synthesized with *Hibiscus rosa-sinensis* L. individually present a spherical morphology (Figure 5), as reported by several authors [8], [41]. FE-SEM reveals too that the AgNPs S5 are in a range of 17-32 nm, the larger AgNPs may be due to the aggregation and agglomeration of the smaller ones as shown in Figure 5. The smallest size found was 17.4 nm.

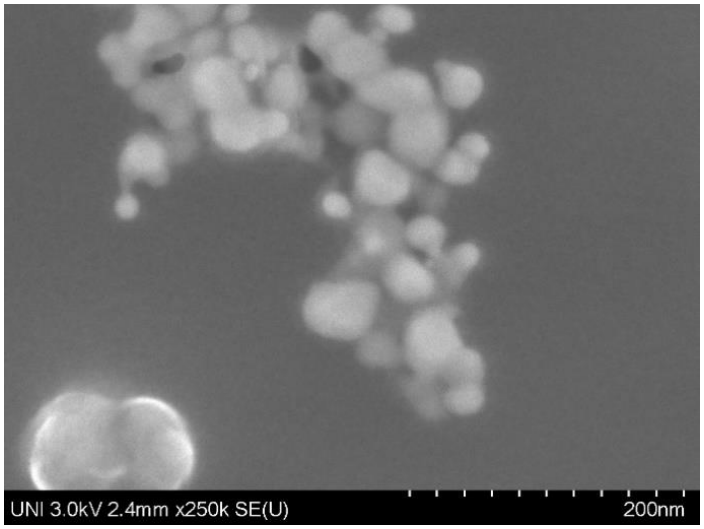

Figure 5. FE-SEM of the AgNPs S5 of petals of *Hibiscus rosa-sinensis* L.

The polydispersity of AgNPs S17 is of the individual spherical type (Figure 6) and its size is between 15 - 26 nm, the smallest size being 15.25 nm.

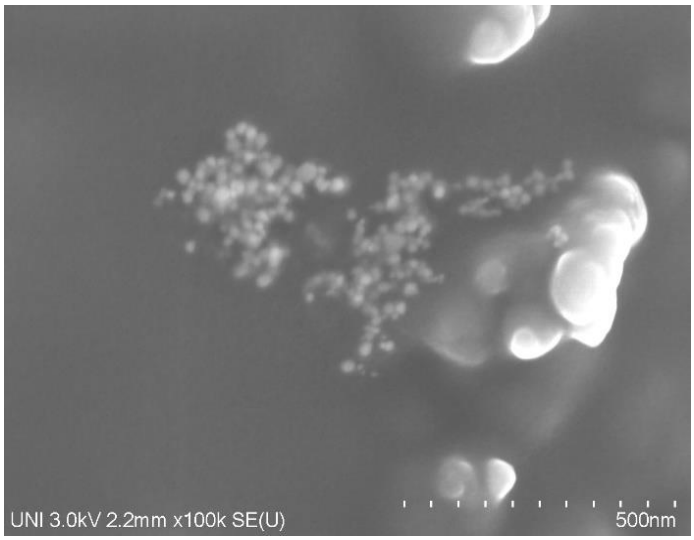

Figure 6. FE-SEM of the AgNPs S17 of petals of *Hibiscus rosa-sinensis* L.

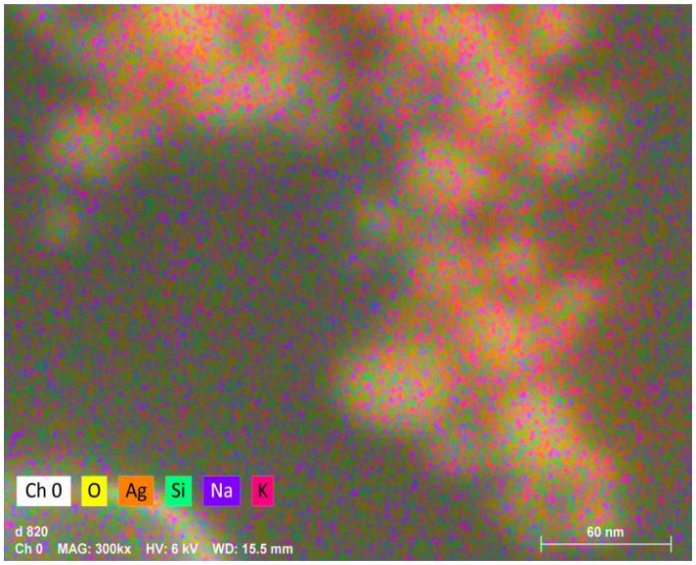

Figure 7. Elemental mapping of Energy Dispersive X-ray Spectroscopy (EDS) of AgNPs synthesized with petal extracts from *Hibiscus rosa-sinensis* L.

EDS analysis at S5 confirmed their elemental composition (Figure 7) showing that silver is the main component, followed by oxygen and potassium in the elemental composition of the AgNPs (Table 9).

Table 9. Identification and percentage of the elemental composition of the S5 AgNPs.

Atomic element	No. Atomic	Neto	Mass [%]	Mass Normal [%]	Atom [%]
Oxygen	8	49572	22.06	32.48	72.55
Silver	47	27504	41.05	60.44	20.02
Silicon	14	2115	0.93	1.37	1.74
Sodium	11	2350	0.50	0.73	1.14
Potassium	19	2571	3.38	4.97	4.55
		Sum	67.92	100.00	100.00

The FTIR spectra of AgNPs S5 and S6 (Figures 8 and 9) allowed to identify the functional groups present.

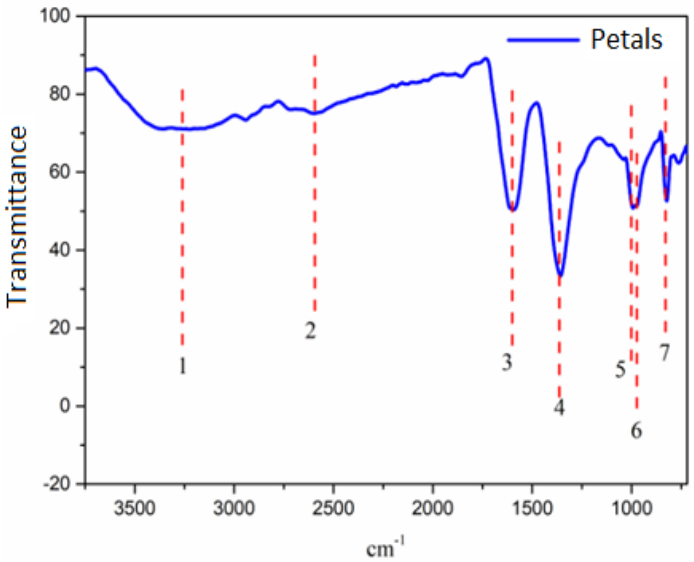

Figure 8. FTIR obtained from AgNPs S5.

Table 10. Signals obtained by FTIR of S5.

N°	cm^{-1}
1	3219.92
2	2594.60
3	1589.70
4	1366.05
5	1004.15
6	974.57
7	827.88

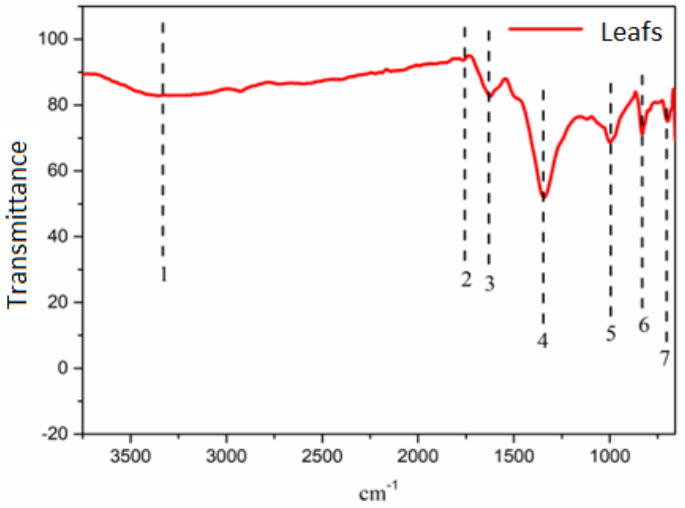

Figure 9. FTIR obtained from AgNPs S6.

Table 11. Signals obtained by FTIR of S6.

N°	cm^{-1}
1	3351.94
2	1762.58
3	1624.39
4	1343.01
5	1005.85
6	843.82
7	661.46

The signals at 3219.92 cm^{-1} and 3351.94 cm^{-1} (-OH) and the signals at 1589.70 cm-1 and 1624.39 cm^{-1} (C=C of aromatic), indicate that no all polyphenols formed nanoparticles during the synthesis. The signals at 1366.05 cm^{-1} and 1343.01 cm^{-1} correspond to the (N-O) bond of $AgNO_3$ [41], [54]. The results confirm that polyphenols are reducers and stabilizers of the synthesized AgNPs.

CONCLUSIONS

Flavonoids were identified from the extract S5 of *Hibiscus rosa-sinensis* L. by UHPLC-ESI-Q-Orbitrap-MS/MS as pelargonidin, petunidin, kaempferol, and orientin, this to the comparison of MS/MS fragmentation with the literature.

Extracts of leaves and flowers (aqueous and ethanolic) proved to be good reducing and stabilizing agents that allowed the synthesis of nanoparticles at different pH, the DLS analysis allowed to determine the polydispersity of the AgNPs synthesized providing agglomeration data and possible precipitation in time, being very useful when selecting the AgNPs for the analysis in FE - SEM.

By FE-SEM analysis, the smallest size of the AgNPs synthesized (17.4 nm) with the ethanol extract of *Hibiscus rosa sinensis* L. petals was determined. The AgNPs synthesized with the aqueous fraction (A) had the smallest size (15.25 nm), demonstrating that the polyphenols present in this fraction are good reducing and stabilizing agents. This technique also allowed to determine the topology of the AgNPs formed (spherical).

AgNPs with a probable size of 42.0 nm were synthesized only with the aqueous fraction of leaves of *Hibiscus rosa sinensis* L.

By IR spectroscopy, the formation of bonds between Ag and the polyphenols present in the ethanol extracts of petals and leaves of *Hibiscus rosa sinensis* L. was confirmed, which supports the probable mechanism of the reaction, it was evidenced as the -OH group coming from the structure of polyphenols is the one that traps the Ag^{+1} ion, reducing it to Ag^0.

ACKNOWLEDGEMENTS

This work was made possible thanks to funding from the Universidad Nacional Federico Villarreal. The authors gratefully acknowledge the Laboratory of Natural Products of the University of Antofagasta, Chile for support in providing the UHPLC-ESI-Q-Orbitrap- MS/MS.

REFERENCES:

1. S. Singh, K. C. Barick, and D. Bahadur, “Surface engineered magnetic nanoparticles for removal of toxic metal ions and bacterial pathogens,” *J. Hazard. Mater.*, vol. 192, no. 3, pp. 1539–1547, 2011, doi: 10.1016/j.jhazmat.2011.06.074.
2. W. R. Li, X. B. Xie, Q. S. Shi, H. Y. Zeng, Y. S. Ou-Yang, and Y. Ben Chen, “Antibacterial activity and mechanism of silver nanoparticles on Escherichia coli,” *Appl. Microbiol. Biotechnol.*, vol. 85, no. 4, pp. 1115–1122, 2010, doi: 10.1007/s00253-009-2159-5.
3. H. M. M. Ibrahim, “Green synthesis and characterization of silver nanoparticles using banana peel extract and their antimicrobial activity against representative microorganisms,” *J. Radiat. Res. Appl. Sci.*, vol. 8, no. 3, pp. 1–11, 2015, doi: 10.1016/j.jrras.2015.01.007.
4. M. del R. Sarmiento, E. Ortiz, and J. Alvarez, “Emergencias ambientales asociadas a sustancias químicas en México,” *Gac. Ecológica, Secr. Medio Ambient. y Recur. Nat.*, no. 66, pp. 54–63, 2003.
5. P. Dong *et al.*, “The green synthesis of Ag-loaded photocatalyst via DBD cold plasma assisted deposition of Ag nanoparticles on N-doped TiO2 nanotubes,” *J. Photochem. Photobiol. A Chem.*, vol. 382, no. March, p. 111971, 2019, doi: 10.1016/j.jphotochem.2019.111971.
6. S. Ahmed, M. Ahmad, B. L. Swami, and S. Ikram, “REVIEW A review on plants extract mediated synthesis of silver nanoparticles for antimicrobial applications : A green expertise,” *J. Adv. Res.*, vol. 7, no. 1, pp. 17–28, 2016, doi: 10.1016/j.jare.2015.02.007.
7. Y. W. Mak, L. O. Chuah, R. Ahmad, and R. Bhat, “Antioxidant and antibacterial activities of hibiscus (Hibiscus rosa-sinensis L .) and Cassia (Senna bicapsularis L .) flower extracts,” *J. King Saud Univ. - Sci.*, vol. 25, no. 4, pp. 275–282, 2013, doi: 10.1016/j.jksus.2012.12.003.
8. D. Philip, “Green synthesis of gold and silver nanoparticles using Hibiscus rosa sinensis,” *Phys. E Low-dimensional Syst. Nanostructures*, vol. 42, no. 5, pp. 1417–1424, 2010, doi: 10.1016/j.physe.2009.11.081.
9. S. M. Seyyednejad, H. Koochak, E. Darabpour, and H. Motamedi, “A survey on Hibiscus rosa-sinensis, Alcea rosea L. and Malva neglecta Wallr as antibacterial agents,” *Asian Pac. J. Trop. Med.*, pp. 351–355, 2010, doi: 10.1016/S1995-7645(10)60085-5.
10. R. Patel, A. Patel, S. Desai, and A. Nagee, “Study of Secondary Metabolites and Antioxidant Properties of Leaves , Stem and Root among Hibiscus Rosa-Sinensis cultivars,” *ASIAN J. EXP. BIOL. SCI.*, vol. 3, no. 4, pp. 719–725, 2015.
11. Z. A. Khan *et al.*, “Antioxidant and antibacterial activities of Hibiscus Rosa-sinensis Linn flower extracts,” *Pak. J. Pharm. Sci.*, vol. 27, no. 3, pp. 469–474, 2014.
12. R. Sharmila Devi and R. Gayathri, “Green Synthesis of Zinc Oxide Nanoparticles by using Hibiscus rosa-sinensis,” *Int. J. Curr. Eng. Technol.*, vol. 4, no. 4, pp. 2444–2446, 2014.
13. D. Nayak, S. Ashe, P. R. Rauta, and B. Nayak, “Biosynthesis, characterisation and antimicrobial activity of silver nanoparticles using Hibiscus rosa-sinensis petals extracts,” *IET Nanobiotechnology*, vol. 9, no. 5, pp. 288–293, 2015, doi: 10.1049/iet-nbt.2014.0047.
14. E. Aguilar and P. Bonilla, “Actividad antioxidante e inmunológica de flavonoides aislados de hojas de Smallanthus sonchifolius (Yacón),” *Cienc. Invest.*, vol. 12, no. 1, pp. 15–23, 2009, [Online]. Available: http://scholar.google.com/scholar?hl=en&btnG=Search&q=intitle:Actividad+antioxidante+e+inmunológica+de+flavonoides+aislados+de+hojas+de+SMALLANTHUS+SONCHIFOLIUS+(YACÓN)#0.
15. G. Rangel and P. Adriana, “Cuantificación de flavonoides (Catequinas) en cáscara de naranja variedad criolla (Citrus sinensis) producida en Norte de Santander,” *LIMENTECH Cienc. Y TECCNOLOGÍA Aliment.*, vol. 8, no. 2, pp. 34–43, 2010.
16. O. Torres, A. Angulo, M. Montaño, and P. Galeano, “ESTUDIO QUIMICO Y OBTENCION DE PRINCIPIOS ACTIVOS DE LA ESPECIE Rollinia,” no. 33, pp. 55–58, 2007.

17. O. R. Lock, *INVESTIGACIÓN FITOQUÍMICA: Métodos en el estudio de productos naturales*. 2016.
18. R. M. Ibrahim, A. M. El-Halawany, D. O. Saleh, E. M. B. El Naggar, A. E. R. O. EL-Shabrawy, and S. S. El-Hawary, "HPLC-DAD-MS/MS profiling of phenolics from securigera securidaca flowers and its anti-hyperglycemic and anti-hyperlipidemic activities," *Brazilian J. Pharmacogn.*, vol. 25, no. 2, pp. 134–141, 2015, doi: 10.1016/j.bjp.2015.02.008.
19. N. A. Begum, S. Mondal, S. Basu, R. A. Laskar, and D. Mandal, "Biogenic synthesis of Au and Ag nanoparticles using aqueous solutions of Black Tea leaf extracts," *Colloids Surfaces B Biointerfaces*, vol. 71, no. 1, pp. 113–118, 2009, doi: 10.1016/j.colsurfb.2009.01.012.
20. F. N. Domenech Gordillo, "Síntesis y caracterización de nanopartículas de plata usando extracto de hojas de Ambrosia arborescens (marco) como reductor químico," 2017.
21. R. Zanella, "Metodologías para la síntesis de nanopartículas : controlando forma y tamaño," *Mundo Nano*, vol. 5, no. 1, pp. 69–81, 2012, doi: http://dx.doi.org/10.22201/ceiich.24485691e.2012.1.45167.
22. S. Ahmed, S. Ullah, M. Ahmad, and B. L. Swami, "Green synthesis of silver nanoparticles using Azadirachta indica aqueous leaf extract," *J. Radiat. Res. Appl. Sci.*, vol. 9, no. 1, pp. 1–7, 2015, doi: 10.1016/j.jrras.2015.06.006.
23. A. T. Madrid Sani, "SÍNTESIS Y CARACTERIZACIÓN DE NANOPARTÍCULAS DE PLATA A PARTIR DE VARIOS EXTRACTOS PIGMENTADOS DE DOS PLANTAS PARA SU APLICACIÓN EN CELDAS SOLARES HÍBRIDAS," 2017.
24. I. Hussain, N. B. Singh, A. Singh, H. Singh, and S. C. Singh, "Green synthesis of nanoparticles and its potential application," *Biotechnol. Lett.*, vol. 38, no. 4, pp. 545–560, 2016, doi: 10.1007/s10529-015-2026-7.
25. C. T. Du and F. J. Francis, "ANTHOCYANINS OF ROSELLE (Hibiscus sabdariffa, L.)," *J. Food Sci.*, vol. 38, no. 5, pp. 810–812, 1973, doi: 10.1111/j.1365-2621.1973.tb02081.x.
26. A. Gärtner, G. Gellerstedt, and T. Tamminen, "Determination of phenolic hydroxyl groups in residual lignin using a modified UV-method," *Nord. Pulp Pap. Res. J.*, vol. 14, no. 2, pp. 163–170, 1999, doi: 10.3183/npprj-1999-14-02-p163-170.
27. M. Barragán Condor, J. M. Aro Aro, A. E. Muñoz Cáceres, and J. Rodríguez Mendoza, "Determinacion de antocianinas y capacidad antioxidante en extractos de (Muehlembeckia volcanica)," *Rev. Investig. Altoandinas - J. High Andean Res.*, vol. 22, no. 2, pp. 161–169, 2020, doi: 10.18271/ria.2020.604.
28. C. J. Vargas Fajardo, "DETERMINACIÓN Y CUANTIFICACIÓN DE COMPUESTOS FENOLICOS EN FLORES DE TARAXACUM OFFICINALE, MEDIANTE HPLC-DAD-MS Y ENSAYOS COLORIMETRICOS UV-VIS.," 2020.
29. H. M. Al-Yousef, W. H. B. Hassan, S. Abdelaziz, M. Amina, R. Adel, and M. A. El-Sayed, "UPLC-ESI-MS/MS Profile and Antioxidant, Cytotoxic, Antidiabetic, and Antiobesity Activities of the Aqueous Extracts of Three Different Hibiscus Species," *J. Chem.*, vol. 2020, 2020, doi: 10.1155/2020/6749176.
30. J. A. M. Fuentes, L. López-Salas, I. Borrás-Linares, M. Navarro-Alarcón, A. Segura-Carretero, and J. Lozano-Sánchez, "Development of an Innovative Pressurized Liquid Extraction Procedure by Response Surface Methodology to Recover Bioactive Compounds from Carao Tree Seeds," *Foods*, vol. 10, no. 2, p. 398, 2021, doi: 10.3390/foods10020398.
31. T. G. García Morales, M. Á. Vásquez Guevara, and S. Lagunas Rivera, "Extracción de antocianinas en los cálices de Hibiscus sabdariffa L. como posible fotosensibilizador.," p. 6, 2019.
32. M. Goutam *et al.*, "Authentication and Photochemical Screening of Hibiscus Rosa Sinensis .," *IJRAR*, vol. 5, no. 4, pp. 712–718, 2018.
48. N. Chandra Lekha and M. Selvipriya, "Green Synthesis of Silver Nanoparticles from aqueous leaves extract of Hibiscus rosa- sinensis and its antioxidant activity," *Kamaraj J. Acad. Res.*, vol. 1, no. 3, pp. 21–28, 2018.
49. M. M. H. Khalil, E. H. Ismail, K. Z. El-baghdady, and D. Mohamed, "Green synthesis of silver nanoparticles using olive leaf extract and its antibacterial activity," *Arab. J. Chem.*, vol. 7, no. 6, pp. 1131–1139, 2014, doi: 10.1016/j.arabjc.2013.04.007.
50. R. Herrera Basurto, B. Simonet Suas, and M. Valcárcel Cases, "Retos de las mediciones en la nanoescala," in *Simposio de metrología*, 2012, pp. 1–6.
51. A. E. Al-Snafi, "Arabian medicinal plants with analgesic and antipyretic effects-plant based review (Part 1)," *IOSR J. Pharm.*, vol. 8, no. 6, pp. 81–102, 2018.
33. J. P. Pérez-Orozco, L. M. Sánchez-Herrera, E. Barrios-Salgado, and M. T. Sumaya-Martínez, "Kinetics of solid-liquid extraction of anthocyanins obtained from Hibiscus rosa-sinensis," *Rev. Mex. Ing. Química*, vol. 12, no. 3, pp. 505–511, 2020, [Online]. Available: http://www.redalyc.org/articulo.oa?id=62029966013.
34. A. Purushothaman, P. Meenatchi, S. S, R. Sundaram, and N. Saravanan, "Quantification of Total Phenolic Content, HPLC Analysis of Flavonoids and Assessment of Antioxidant and Anti-haemolytic Activities of Hibiscus rosa-sinensis L. Flowers in vitro," *Int. J. Pharma Res. Heal. Sci.*, vol. 4, no. 5, pp. 134–50, 2016, doi: 10.21276/ijprhs.2016.05.02.
35. L. B. D. S. Nascimento, A. Gori, A. Raffaelli, F. Ferrini, and C. Brunetti, "Phenolic compounds from leaves and flowers of hibiscus roseus: Potential skin cosmetic applications of an under-investigated species," Plants, vol. 10, no. 3, pp. 1–16, 2021, doi: 10.3390/plants10030522.
36. .H. Z. Lina, M. M. Samy, A. E. B. Samir, A. M. Fatma, M. T. Kawther, and A. S. Abdelaaty, "Hypoglycemic and antioxidant effects of Hibiscus rosa-sinensis L. leaves extract on liver and kidney damage in streptozotocin induced diabetic rats," *African J. Pharm. Pharmacol.*, vol. 11, no. 13, pp. 161–169, 2017, doi: 10.5897/ajpp2017.4764.
37. [C. Y. Kuo, E. S. Kao, K. C. Chan, H. J. Lee, T. F. Huang, and C. J. Wang, "Hibiscus sabdariffa L. extracts reduce serum uric acid levels in oxonate-induced rats," *J. Funct. Foods*, vol. 4, no. 1, pp. 375–381, 2012, doi: 10.1016/j.jff.2012.01.007.
38. L. P. Guan and B. Y. Liu, "Antidepressant-like effects and mechanisms of flavonoids and related analogues," *Eur. J. Med. Chem.*, vol. 121, pp. 47–57, 2016, doi: 10.1016/j.ejmech.2016.05.026.
39. N. Vasudeva and S. K. Sharma, "Biologically active compounds from the genus Hibiscus," *Pharm. Biol.*, vol. 46, no. 3, pp. 145–153, 2008, doi: 10.1080/13880200701575320.
40. H. Y. Chai, S. M. Lam, and J. C. Sin, "Green synthesis of magnetic Fe-doped ZnO nanoparticles via Hibiscus rosa-sinensis leaf extracts for boosted photocatalytic, antibacterial and antifungal activities," *Mater. Lett.*, vol. 242, pp. 103–106, 2019, doi: 10.1016/j.matlet.2019.01.116.
41. S. Surya, G. Dinesh Kumar, and R. Rajakumar, "Green Synthesis of Silver Nanoparticles from Flower Extract of Hibiscus rosa-sinensis and Its Antibacterial Activity," *Int. J. Innov. Res. Sci. Eng. Technol. (An ISO*, vol. 5, no. 4, pp. 5242–5247, 2016, doi: 10.15680/IJIRSET.2016.0504129.
42. A. Santos-Espinoza, F. Gutiérrez-Miceli, V. Ruíz-Valdiviezo, and J. Montes-Molina, "El papel de los compuestos polifenólicos en la síntesis verde de nanopartículas metálicas," *BioTecnología*, vol. 24, no. 2, p. 46, 2020.
43. K. Vijayaraghavan and S. P. K. Nalini, "Biotemplates in the green synthesis of silver nanoparticles," *Biotechnol. J.*, vol. 5, no. 10, pp. 1098–1110, 2010, doi: 10.1002/biot.201000167.
44. D. Garg, A. Shaikh, A. Muley, and T. Marar, "In-vitro antioxidant activity and phytochemical analysis in extracts of Hibiscus rosa-sinensis stem and leaves," *Free Radicals Antioxidants*, vol. 2, no. 3, pp. 41–46, 2012, doi: 10.5530/ax.2012.3.6.
45. A. Shehzad *et al.*, "Synthesis, characterization and antibacterial activity of silver nanoparticles using Rhazya stricta," *PeerJ*, vol. 2018, no. 12, pp. 1–15, 2018, doi: 10.7717/peerj.6086.
46. K. Vijayaraghavan and T. Ashokkumar, "Plant-mediated biosynthesis of metallic nanoparticles: A review of literature, factors affecting synthesis, characterization techniques and applications," *J. Environ. Chem. Eng.*, vol. 5, no. 5, pp. 4866–4883, 2017, doi: 10.1016/j.jece.2017.09.026.
47. K. Muthu and S. Priya, "Green synthesis, characterization and catalytic activity of silver nanoparticles using Cassia auriculata flower extract separated fraction," *Spectrochim. Acta - Part A Mol. Biomol. Spectrosc.*, vol. 179, pp. 66–72, 2017, doi: 10.1016/j.saa.2017.02.024.
52. D. Alvear, S. Galeas, and A. Debut, "Síntesis y Caracterización de Nanopartículas de Magnetita," *Rev. Politécnica*, vol. 39, no. 2, pp. 61–66, 2017, doi: 10.33333/rp.v39i2.545.
53. S. Ahmed, Annu, S. A. Chaudhry, and S. Ikram, "A review on biogenic synthesis of ZnO nanoparticles using plant extracts and microbes: A prospect towards green chemistry," *J. Photochem. Photobiol. B Biol.*, vol. 166, pp. 272–284, 2017, doi: 10.1016/j.jphotobiol.2016.12.011.
54. L. Katata-Seru, T. Moremedi, O. S. Aremu, and I. Bahadur, "Green synthesis of iron nanoparticles using Moringa oleifera extracts and their applications: Removal of nitrate from water and antibacterial activity against Escherichia coli," *J. Mol. Liq.*, vol. 256, pp. 296–304, 2018, doi: 10.1016/j.molliq.2017.11.093.